

The Effect of FTO Sheet Resistance on the Efficiency of Dye Sensitized Solar Cell

Nabeel A. Bakr^{*}, AbdulRahman K. Ali^{**}, and Shaimaa M. Jassim^{*}

^{*} Department of Physics, College of Science, University of Diyala, Diyala, Iraq

^{*} Department of Applied Science, University of Technology, Baghdad, Iraq

^{*} Email: nabeelalibakr@yahoo.com

Abstract

In this work, DSSCs have been fabricated successfully using a simple procedure without the need for any complicated facilities. The XRD analysis of the TiO₂ film confirmed that it has a polycrystalline structure belonging to anatase phase with crystallite size of 12.4 nm. UV-Vis spectroscopy was used to characterize the absorbance spectrum of the TiO₂ film and Z907 dye. The energy gap of the TiO₂ film estimated by Tauc's plot was 3.12 eV. The SEM micrograph of the TiO₂ film shows that the layer has a spongy shape with reduction in the number of open pores making easy for dye adsorption and electron transport. The AFM micrograph and the granularity cumulative distribution chart of the TiO₂ film shows that the average roughness, root mean square roughness and average grain size were about 0.356 nm, 0.423 nm and 82.48 nm respectively. The DSSC fabricated using glass substrates coated with 8 Ω/□ sheet resistance FTO achieved the highest short circuit density (J_{SC}) and conversion efficiency (η) of 4.069 mA/cm² and 1.786 %, respectively. Subsequently, the enhancement in efficiency was ~ 84 % compared with the conversion efficiency of DSSC fabricated using glass substrates coated with 15 Ω/□ sheet resistance FTO.

Keywords: DSSC, Z907 Dye, TiO₂ Layer, FTO Sheet Resistance, Efficiency Enhancement

Introduction:

Energy is one of the most important factors to influence human life in the 21st century. The great increasing consumption of fossil fuels, causing global warming and environmental pollution, has led to a greater focus on renewable energy sources and sustainable development [1]. The sun's energy is the primary source for most energy forms found on the earth. Solar energy is clean, abundant and renewable [2]. The dye-sensitized solar cell (DSSC) is a device for the conversion of solar energy into electrical energy [3]. Dye-sensitized solar cell (DSSC) which was invented by Gratzel in 1991 also known as (Gratzel Cell), which is characterized as light-weight, flexibility, workability under low-light, conditions, conformability, portable, inexpensive, low toxicity and transparent relative to conventional solid state solar cells [4,5]. The basic structure of DSSC is composed of two conductive transparent glasses coated with a Transparent Conductive Oxide (TCO) substrate, TiO_2 nanoparticle layer, dye molecules, an electrolyte and a transparent film of platinum catalyst in a sandwich structure [6] as shown in figure (1). The actual color of the cell is mainly due to the superposition of the optical spectra of the electrolyte and the dye [7]. There are factors effected on the cell efficiency such as series resistance of substrate, is an important parameter for determining the efficiency [8]. TEC-8 or TEC -15 substrates, the value of 8 or 15 refers to the sheet resistance. The sheet resistance is about 8-15 Ω /square with a transmittance of 80-85% in the visible region [9]. Fluorine doped tin oxide (FTO) coated on glass substrate, is a widely used choice for the transparent conducting glass. Fluorine doped tin oxide (FTO) exhibits good visible transparency owing to its wide bandgap [10]. FTO is mechanically, chemically, electrochemically stable and high electrical conductivity, and it is utilized in many of technologies including; dielectric layers in low emissivity coatings for windows, gas sensor devices and thin film solar cells [11]. Solar cell that used FTO films is DSSC. FTO film is used to collect electrons from the sensitized dye [12].

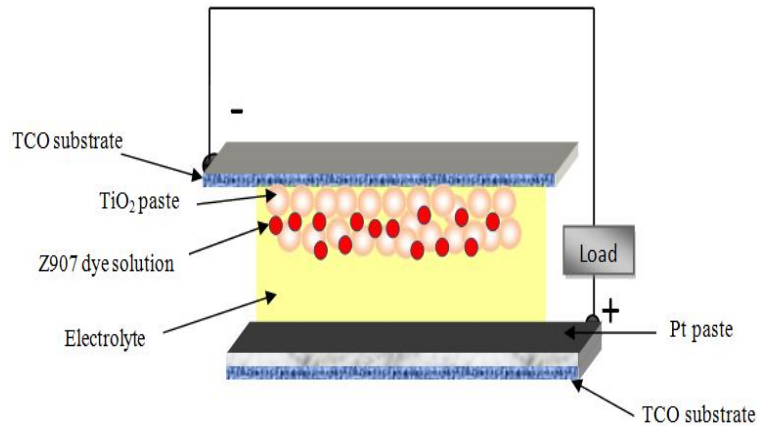


Fig. 1. Schematic diagram of DSSC basic structure.

The aim of this work is to prepare a dye sensitized solar cell by Doctor-Blade method and investigate the effect different TEC substrate on the power conversion efficiency (η) of the prepared solar cell.

Experimental Procedure:

All the materials used in this work were supplied by Dyesol Company/Australia. The materials were as follows: Fluorine Tin Oxide (FTO) (sheet resistance $8 \Omega/\text{sq}$ and $15 \Omega/\text{sq}$) coated glass substrates, TiO_2 paste (18-NRT), Z907 dye, organic solvent based electrolyte (EL-HSE), platinum paste, hot- melted, Acetone, distilled water.

For the preparation of the photoanode, FTO glass substrate with size of ($2.5 \text{ cm} \times 2.5 \text{ cm}$) was used. The FTO glass was cleaned in ultrasonic bath for 5 minutes in distilled water and for 5 minutes in acetone. The TiO_2 paste was deposited on FTO glass by Doctor-blade method and the thickness of the titania layer was determined by the thickness of scotch tape which has a thickness of $10 \mu\text{m}$ placed on the right and left sides of the conductive face of substrate. Then the scotch tape was removed and the films were left to dry for 30 minutes in a covered Petridish. Thereafter, the films were annealed at $550 \text{ }^\circ\text{C}$ for 30 minutes in ambient atmosphere. Finally, the photoanodes were allowed to cool at room temperature. After cooling, the

photoanodes were immersed in a 0.25 mM Z907 dye solution for 24 hours. For the preparation of the counter electrode, two holes of 1 mm diameter were drilled to enable a later injection of electrolyte and platinum (Pt) paste was deposited on conductive side of FTO glass by Doctor-blade method, and the electrodes were then annealed at 450 °C for 30 minutes in ambient atmosphere. This leads to homogenous distributed platinum with good catalytic activity. The photoanode and counter electrode were assembled into a sandwich structure using hot-melted, with a thickness of 30 μm as spacer. The sealant gasket was placed around TiO₂ paste and the counter electrode was put on it while the Pt film faces the TiO₂. Finally, few drops of the electrolyte were injected through the holes in the counter electrode by a pipette, and the holes were sealed by plaster to prevent evaporation.

The crystallite phase of TiO₂ was identified by X-ray diffractometer (Shimadzu 6000, Japan) using CuKα radiation (λ= 1.5406 Å). The surface morphology of TiO₂ was investigated by SEM (JSM-7000F) type. The UV–Vis absorption spectra of the TiO₂ film and Z907 dye were measured by UV–VIS–NIR spectrophotometer (Shimadzu, UV-1800). The photovoltaic performance of the DSSCs was measured using Keithley 2400 multimeter and tungsten halogen lamp. Based on I–V curve, the fill factor (FF) was calculated according to the formula:

$$FF = \frac{J_{max} \cdot V_{max}}{J_{sc} \cdot V_{oc}} \quad (1)$$

Where J_{max} is the maximum photocurrent density, V_{max} is maximum photovoltage, J_{sc} is the short circuit photocurrent density and V_{oc} is the open-circuit photovoltage. The photoelectric conversion efficiency (η) was calculated according to the following equation:

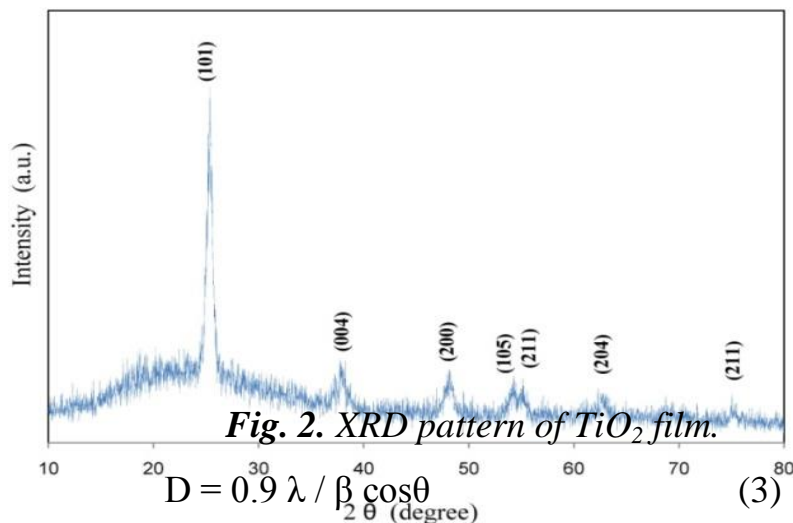
$$\eta (\%) = \frac{J_{sc} \cdot V_{oc} \cdot FF}{P_{in}} = \frac{J_{max} \cdot V_{max}}{P_{in}} \quad (2)$$

Where P_{in} is the incident power.

Results and Discussion:

1- Structural Analysis

Crystalline characterizations of TiO₂ film prepared by Doctor-blade method on glass substrate were carried out by X-ray diffraction (XRD). Figure (2) shows the XRD diffraction pattern of the TiO₂ film annealed at 550 °C. From the figure, it was confirmed that the TiO₂ layer material has anatase phase with polycrystalline structure according to the ICDD standard card no. (21-1272) [13]. The diffraction peaks were indexed to the crystal planes (101), (004), (200), (105), (211), (204) and (215) and this result is in agreement with the results reported by Wang et al. [14]. The highest and strongest peak of TiO₂ film was at $2\theta \approx 25.4^\circ$ corresponding to (101) direction. The crystallite size of TiO₂ film was calculated by Scherrer's formula given by the following equation [15]:



Where D is the crystallite size, λ is the X-ray wavelength of Cu K α radiation, β is the full width at half maximum (FWHM) and θ is the Bragg's angle. The lattice parameters of the TiO₂ film are $a = 3.781 \text{ \AA}$ and $c = 9.477 \text{ \AA}$, which are in agreement with the standard values (i.e., $a = 3.785 \text{ \AA}$ and $c = 9.513 \text{ \AA}$) and the crystallite size is 12.4 nm.

2- Morphological analysis

The surface morphology of TiO₂ film was characterized by SEM. Figure (3) displays the SEM image of TiO₂ film of 10 μm thickness which has been deposited on the FTO glass after annealing at 550 °C for 30 minutes. The SEM micrograph shows a spongy shape with reduction in the number of open pores making easy for dye adsorption and electron transport [16]. The average particle size of TiO₂ NPs is about 20-40 nm. The small particles of TiO₂ film have larger surface area and subsequently absorb more dye molecules and this may lead to improved DSSC performance.

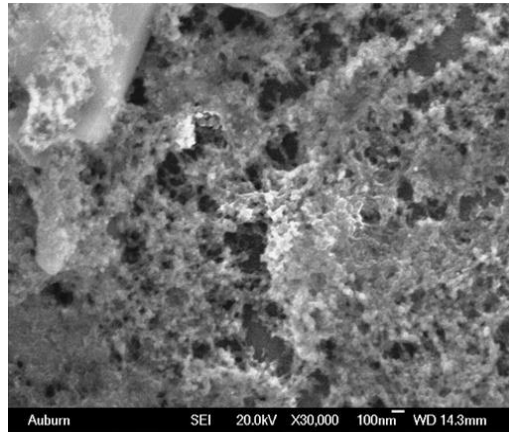


Fig. 3. SEM image of TiO₂ film at 30,000X.

3- (AFM) Results

The surface topography of TiO₂ film prepared by Doctor-blade method on FTO glass was studied by Atomic Force Microscope (AFM) technique. The 3-D AFM image and granularity cumulative distribution chart of TiO₂ film annealed at 550 °C for 30 minutes are shown in figures (4a) and (4b) respectively. The average roughness, root mean square roughness and grain size of the TiO₂ film were about 0.356 nm, 0.423 nm and 82.48 nm respectively.

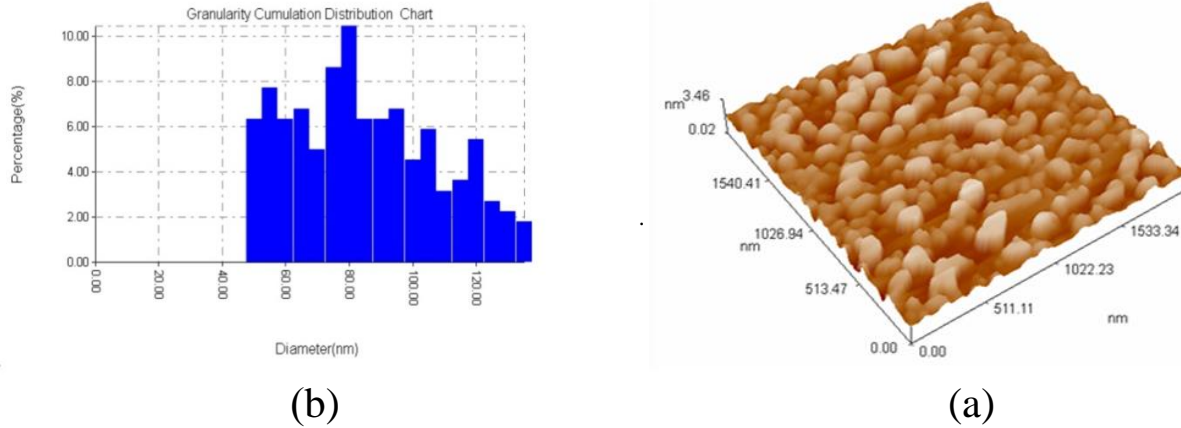


Fig. 4 (a) 3-D AFM image and (b) Granularity Cumulative Distribution chart of TiO₂ film.

4- Optical properties

Figure (5) demonstrates the UV–Vis absorption spectrum of Z907 dye solution in the wavelength range of (350–800) nm. From the figure, it can be seen that the dye has two absorption peaks at around (428 and 542 nm).

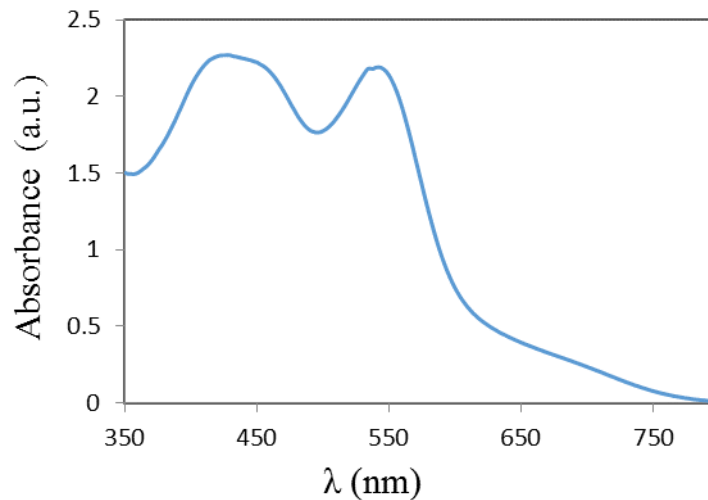


Fig.5. UV-Vis absorption spectra of Z907 dye.

Figure (6) illustrates the UV–Vis absorption spectrum of TiO₂ film annealed at 550 °C. From the figure, it can be noticed that the film has clear and sharp absorption edge at wavelength of ~ 350 nm. The direct band gap of the TiO₂ film was determined by plotting $(\alpha h\nu)^2$ vs. $h\nu$. The optical band gap E_g value is

estimated by extrapolation of the straight-line portion of the plot to zero absorption edge as shown in Figure (7). From the figure, it was observed that direct optical band gap for annealed TiO₂ film was 3.12 eV.

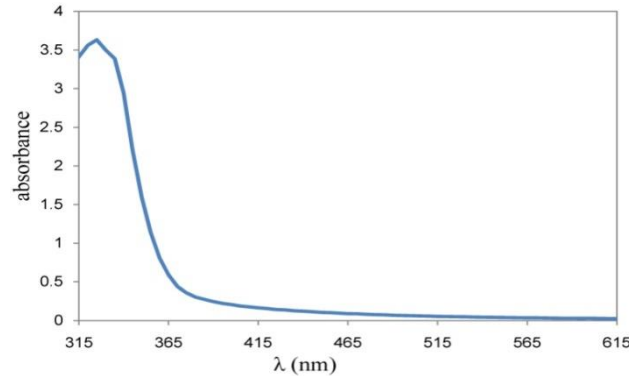


Fig.6. UV-Vis absorption spectra of TiO₂ layer.

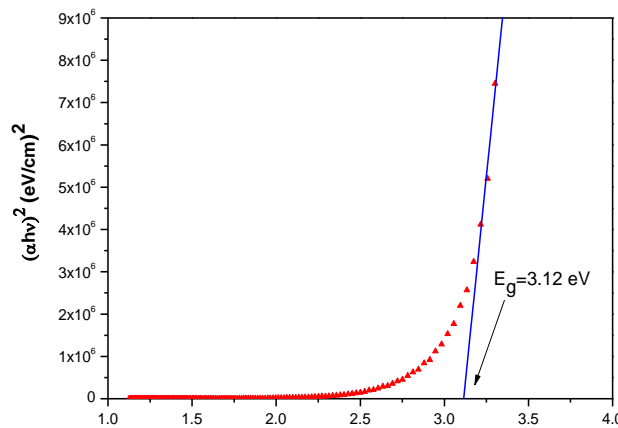


Fig.7. Tauc's plot of TiO₂ film.

5- Current voltage characteristics

The DSSCs fabricated by using TiO₂ films with thickness of 10 μm annealed at 550 °C for 30 minutes and Z907 dye as sensitizer with concentration 0.25 mM. Figure (8) demonstrates the J-V characteristics of two DSSCs based on TEC substrates of different resistances. It was observed that the DSSC with TEC-8 Ω has current density-voltage curve area larger than that of the DSSC with TEC-15 Ω. It was also noted that J_{SC} increases for DSSC with TEC-8 Ω compared to that of DSSC with TEC-15 Ω, while V_{OC} remains unchanged. Subsequently, an increase in short circuit current density leads directly to an increase in the energy conversion

efficiency. This can be ascribed to difference in the thickness of Fluorine Tin Oxide (FTO) layer, TEC-8 Ω is 600 nm thick while TEC-15 Ω is 300 nm thick (i.e. that the series resistance of TEC-8 Ω lower compared TEC-15). The photovoltaic parameters of the DSSCs prepared using different TEC substrates are summarized in Table (1). The efficiency of the DSSC prepared by using TEC-8 Ω enhanced ~ 84 % compared to the DSSC prepared by using TEC-15 Ω .

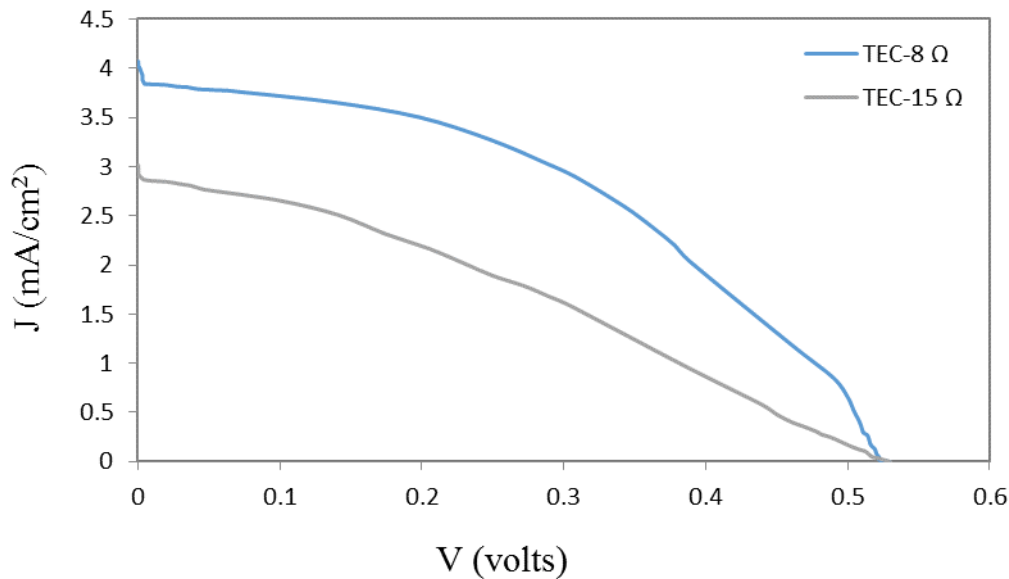


Fig. 8. J-V curves of DSSCs using different TEC substrates.

Table (1): The photovoltaic parameters of DSSCs fabricated using different TEC substrates.

Substrate Type	V_{OC} (V)	J_{SC} (mA/cm ²)	V_{max} (V)	J_{max} (mA/cm ²)	FF	η (%)
TEC-15 Ω	0.53	3.011	0.289	1.682	0.305	0.972
TEC-8 Ω	0.53	4.069	0.31	2.881	0.414	1.786

Conclusions:

DSSCs with TEC-8 Ω and 15 Ω substrates have been fabricated successfully using a simple procedure without the need for any complicated facilities. The absorption spectra in the wavelength range of (350-750) nm show that Z907 dye has two peaks. The conversion efficiency of the DSSC prepared with TEC-8 Ω about 1.786 % which represents an enhancement of ~ 84 % compared to the DSSC efficiency prepared by TEC-15 Ω .

References

- [1] C. Cai, S. Tseng, M. Kuo, K. A. Lin, H. Yang, and R. Lee, "Photovoltaic Performance of N719 Dye based Dye-sensitized Solar Cell with Transparent Macroporous Anti-Ultraviolet Photonic Crystal Coatings", RSC Advances, Vol. 5, pp. 1-29, (2015).
- [2] N. A. Omair, S. M. Reda, F. M. Al-Hajri, "Effect of Organic Dye on the Photovoltaic Performance of Dye-Sensitized ZnO Solar Cell", Advances in Nanoparticles, Vol. 3, pp. 31-35, (2014).
- [3] J. Deenathayalan, M. Saroja, M. Venkatachalam, P. Gowthaman, "ZnO Nanorod based Dye Sensitized Solar Cells with Natural Dyes Extracted from AmaranthusCaudatus and Morus Alba", Journal of NanoScience and NanoTechnology, Vol. 2, No. 4, pp. 384-389, (2014).
- [4] A. Fakharuddin, R. Jose, T. M. Brown, F. F. Santiago, Juan Bisquert, "A perspective on the production of dye-sensitized solar modules", Energy Environmental Science, Vol. 7, pp. 3952–3981, (2014).
- [5] A. A. Khafaji, D. B. Alwan, F. H. Ali, W. A. A. Twej, "Influence of grain size, electrode type and additives on dye sensitized solar cells efficiency", Environmental Science: An Indian Journal, Vol. 12, No. 6, pp. 217-223 (2016).
- [6] K. Guo, M. Li, X. Fang, X. Liu, B. Sebo, Y. Zhu, Z. Hu, X. Zhao, "Preparation and enhanced properties of dye-sensitized solar cells by surface

- plasmon resonance of Ag nanoparticles in nanocomposite photoanode", *Journal of Power Sources*, Vol. 230, pp. 155-160, (2013).
- [7] R. Tagliaferro, D. Colonna, T. M. Brown, A. Reale, A. D. Carlo, "Interplay between transparency and efficiency in dye sensitized solar cells", *Optics Express*, Vol. 21, No. 3, pp. 3235-3242, (2013).
- [8] R. Escalante, D. Pourjafari, D. Reyes-Coronado, G. Oskam, "Dye-sensitized solar cell scale-up: Influence of substrate resistance", *Journal of renewable and sustainable energy*, Vol. 8, No. 2, pp. 1-10, (2016).
- [9] F. Santiagoa, F. Bisquert, J. Palomares, E. Haque, S. A. Durrant, J. R. "Impedance spectroscopy study of dye-sensitized solar cells with undoped spiro-OMeTAD as hole conductor", *Journal Applied Physics*, Vol. 100, No. 3, pp. 1-7, (2006).
- [10] G. R. A. Kumara, C. S. K. Ranasinghe, E. N. Jayaweera, H. M. N. Bandara, M. Okuya, R. M. G. Rajapakse, "Substrates by Atomized Spray Pyrolysis Technique and Their Subsequent Use in Dye-Sensitized Solar Cells", *The Journal of Physical Chemistry C*, Vol. 118, No. 30, pp. 16479-16485, (2014).
- [11] M. L. M. Napi, M. F. Maarof, C. F. Soon, N. Nayan, F. I. M. Fazli, N. K. A. Hamed, S. M. Mokhtar, N. K. Seng, M. K. Ahmad, A. B. Suriani, A. Mohamed, "Fabrication of Fluorine Doped Tin Oxide (FTO) Thin Films Using Spray Pyrolysis Deposition Method for Transparent Conducting Oxide", *Journal of Engineering and Applied Sciences*, Vol. 11, No. 14, pp. 8800-880, (2016).
- [12] S. Ngamsinlapasathian, A. Kitiyanan, T. Fujieda, and S. Yoshikawa, "Effect of Substrates on Dye-Sensitized Solar Cell Performance Using Nanocrystalline TiO_2 ", *ECS Transactions*, Vol. 1, No. 33, pp. 7-15, (2006).
- [13] R. Vijayalakshmi and V. Rajendran, "Synthesis and characterization of nano- TiO_2 via different methods", *Archives of Applied Science Research*, Vol. 4 (2), pp. 1183-1190, (2012).

- [14] Y. Wang, L. Li, X. Huang, Q. Lia and G. Li, "New insights into fluorinated TiO₂ (brookite, anatase and rutile) nanoparticles as efficient photocatalytic redox catalysts", RSC Advances, Vol. 5, No. 43, pp. 34302-34313, (2015).
- [15] C. H. Wei and C.M. Chang, "Polycrystalline TiO₂ thin films with different thicknesses deposited on unheated substrates using RF magnetron sputtering", Materials Transactions, Vol. 52, No.3, pp. 554-559, (2011).
- [16] H. Sh. Wu, and Y. L. Wang, "Effects of annealing temperature on the structure and properties of TiO₂ nanofilm materials", Advanced Materials Research, Vol. 531, pp. 203-206, (2012).